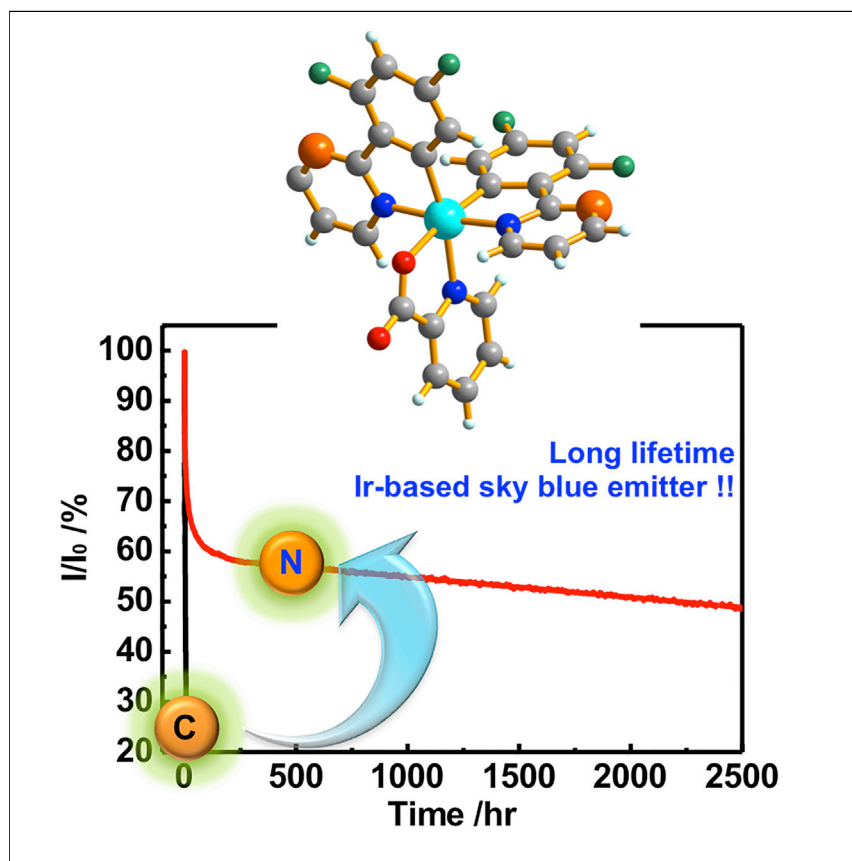


Article

Anomalously Long-Lasting Blue PhOLED Featuring Phenyl-Pyrimidine Cyclometalated Iridium Emitter



Blue phosphorescent material with both high efficiency and long durability is a long-standing challenge in the field of organic light-emitting devices (OLEDs). This work describes an anomalously blue phosphorescent OLED featuring the phenyl-pyrimidine cyclometalated iridium emitter, which has nearly unitary emission quantum yield, strong horizontal emitting dipole orientation, and short excited-state lifetime to ensure high electroluminescence efficiency and a long device operation lifetime of $T_{50} > 2,200$ hr.

Monima Sarma, Wei-Lung Tsai,
Wei-Kai Lee, ..., Shih-Hung Liu,
Pi-Tai Chou, Ken-Tsung Wong

wucc@ntu.edu.tw (C.-C.W.)
chop@ntu.edu.tw (P.-T.C.)
kenwong@ntu.edu.tw (K.-T.W.)

HIGHLIGHTS

Efficient and stable blue phosphorescent pyrimidine cyclometalated iridium complex

~100% PLQY, short excited-state lifetime, and horizontal emitting dipole

Efficient EL with external quantum efficiency >31% and very small efficiency roll-off

Anomalously long device operation lifetime of $T_{50} > 2,200$ hr



Sarma et al., Chem 3, 461–476
September 14, 2017 © 2017 Elsevier Inc.
<http://dx.doi.org/10.1016/j.chempr.2017.08.001>

Article

Anomalously Long-Lasting Blue PhOLED Featuring Phenyl-Pyrimidine Cyclometalated Iridium Emitter

Monima Sarma,^{1,5} Wei-Lung Tsai,^{2,5} Wei-Kai Lee,² Yun Chi,³ Chung-Chih Wu,^{2,*} Shih-Hung Liu,¹ Pi-Tai Chou,^{1,*} and Ken-Tsung Wong^{1,4,6,*}

SUMMARY

Simply replacing pyridine in cyclometalating ligands in **Irpic** with pyrimidine affords the complex **MS 2**, which has a slight red-shifted emission but shorter excited-state lifetime and the capability to form a highly efficient blue phosphorescent organic light-emitting device (OLED) with long operation lifetime ($T_{50} > 2,200$ hr). Further replacement of the picolinate-based ancillary ligand of **MS 2** with strong-field CF_3 -containing pyridine-azole ancillary ligands leads to bluer emitters (**MS 17** and **MS 19**) with nearly unitary photoluminescence quantum yield and preferential horizontal emitting dipole orientations (with horizontal dipole ratios of 75%–77%) beneficial for OLED optical out-coupling. OLEDs using **MS 17** and **MS 19** as emitters gave bluer emission and very high external quantum efficiency exceeding 31% yet with comparably short device lifetimes as **Irpic**-based devices. Theoretical analysis indicates that the distinct stability of the **MS 2**-based device might be attributed to its relatively large energy difference between ^3MC (metal center d-d transition) and $^3\text{MLCT}$ states.

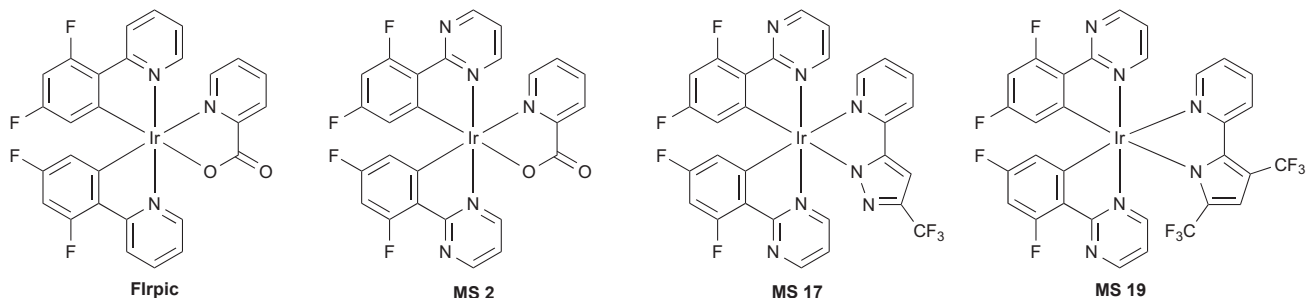
INTRODUCTION

Organic light-emitting diodes (OLEDs) have emerged as an important next-generation display and lighting technology.^{1–4} One of the key factors for achieving highly efficient OLEDs is to effectively harvest electrically generated excitons. Because of the strong spin-orbit coupling effect, metal-centered phosphorescent emitters allow both singlet and triplet excitons to be utilized for electroluminescence (EL),^{5,6} providing the capability for 100% internal quantum efficiency.^{7–10} Among various metal-containing phosphors, cyclometalated iridium(III) complexes are considered to be one of the most promising triplet emitters because of their versatile color tunability as well as high photoluminescence quantum yield (PLQY).^{11–17} Efficient and stable red and green Ir-based phosphorescent materials have been successfully introduced into commercial OLED displays. Yet, practical applications of blue-emitting Ir(III) complexes still lag behind, mostly because of stability issues. Up to this stage, the development of Ir-based blue phosphorescent materials with superior efficiency and stability remains a challenge.¹⁷

En route to true-blue Ir-based phosphorescent materials, increased emitting-state energy is inevitable, which could eventually arise in the proximity of the metal-centered d-d state and result in either quenching of emission or ligand dissociation.^{10,17} These processes can be avoided by utilizing chelates with larger ligand field strengths, i.e., ligands capable of forming stronger metal-ligand coordination to destabilize the metal-centered d-d excited states.¹⁰ In the development of

The Bigger Picture

Blue problem! Vivid displays and pseudo-natural lighting adopting OLED technology have started to benefit our daily life. Earlier OLEDs using fluorescent emitters yielded only 25% emissive singlet but 75% non-emissive and wasted triplet excitons. With the invention of phosphorescent iridium complexes, both singlet and triplet excitons can be effectively harvested for emission with the aid of spin-orbit coupling, yielding much more efficient electroluminescence and triggering commercialization of OLED technology. Currently, red and green devices in active-matrix OLED displays have Ir-based phosphorescent emitters. For further improvement of OLED display efficiency, stable Ir-based blue materials are essential. This “blue problem” is a long unresolved challenge. This work presents a good example of a high-efficiency and long-lasting Ir-based blue emitter, which could open a new window for possible solutions to the long-standing “blue problem” in OLEDs.



Scheme 1. Structures for the Complexes Flrpic, MS 2, MS 17, and MS 19

blue-emitting Ir(III) complexes,^{18–28} immense credit must be given to Adachi et al.;¹⁸ the pyridine-containing sky blue emitter Flrpic, bis[2-(4,6-difluorophenyl)pyridinato-C²,N](picolinato)iridium(III) developed by them remains an ubiquitous and benchmarking prototype. However, as a benchmark blue phosphor for high-performance phosphorescent OLEDs (PhOLEDs), Flrpic has certain shortcomings that are common to many reported blue phosphorescent emitters. These include unsatisfactory CIE color coordinates for full-color displays, significant efficiency roll-off at higher brightness, and short device operating lifetimes,^{29–33} the improvement of which remains essential and critical for OLED applications. In this work, we explore the potential of replacing difluorophenyl-pyridine (dfppy), which is commonly used as the cyclometalating ligand for blue-emitting Ir complexes (e.g., Flrpic), with the diazine-containing ligand, difluorophenyl-pyrimidine (dfppm), affording compound **MS 2** (Scheme 1). Phosphorescent Ir complexes with dfppm as the cyclometalating ligand, including **MS 2**, had been reported previously.^{29–31} Unfortunately, with rather preliminary characterizations and inferior EL efficiencies in previous reports, the potential of such Ir complexes was substantially underestimated, and they failed to arouse sufficient attention and interest. Our studies elaborated here revitalize this class of Ir complexes as excellent phosphorescent emitters in OLEDs. Yet, according to our own studies and previous reports,^{29–31} diazine-containing cyclometalating ligands tend to cause red-shifted emission in comparison with their pyridine-based counterparts. To offset this effect and to obtain bluer emission, strong-field ancillary CF₃-containing pyridine-azole ligands, such as 2-(3-(trifluoromethyl)-1H-pyrazol-5-yl)pyridine³² and 2-(3,5-bis(trifluoromethyl)-1H-pyrrol-2-yl)pyridine,³³ are further adopted to afford the compounds **MS 17** and **MS 19** (Scheme 1), respectively, giving more blue-shifted emission than with Flrpic. Comprehensive and comparative (cf. Flrpic) studies were conducted for these Ir complexes in terms of structural, physical, photophysical, and EL properties. All titled Ir complexes are efficient blue emitters with nearly unitary PLQYs and preferential horizontal emitting dipole orientations (with horizontal dipole ratios of 75%–77%). Among these complexes, blue OLED based on **MS 2** displays an outstandingly long operation lifetime ($T_{50} > 2,200$ hr), and the bluest emission and high external quantum efficiency (EQE) exceeding 31% can be attained from the OLED based on **MS 17**.

RESULTS AND DISCUSSION

Although **MS 2** is a reported complex, previous characterization and understanding of its properties, including physical and electroluminescent properties, were surprisingly preliminary. The physical properties of **MS 2** are thus carefully re-examined here. From the absorption edge (Figure 1A) at 470 nm for **MS 2**, the corresponding optical energy gap (E_g) was estimated to be 2.64 eV, which is slightly smaller than that (2.67 eV) of Flrpic. **MS 2** exhibits a slightly red-shifted (~5 nm) emission peak

¹Department of Chemistry, National Taiwan University, Taipei 10617, Taiwan

²Department of Electrical Engineering, Graduate Institute of Electronics Engineering and Graduate Institute of Photonics and Optoelectronics, National Taiwan University, Taipei 10617, Taiwan

³Department of Chemistry, National Tsing Hua University, Hsinchu 300, Taiwan

⁴Institute of Atomic and Molecular Science Academia Sinica, Taipei 10617, Taiwan

⁵These authors contributed equally

⁶Lead Contact

*Correspondence: wucc@ntu.edu.tw (C.-C.W.), chop@ntu.edu.tw (P.-T.C.), kenwong@ntu.edu.tw (K.-T.W.)

<http://dx.doi.org/10.1016/j.chempr.2017.08.001>

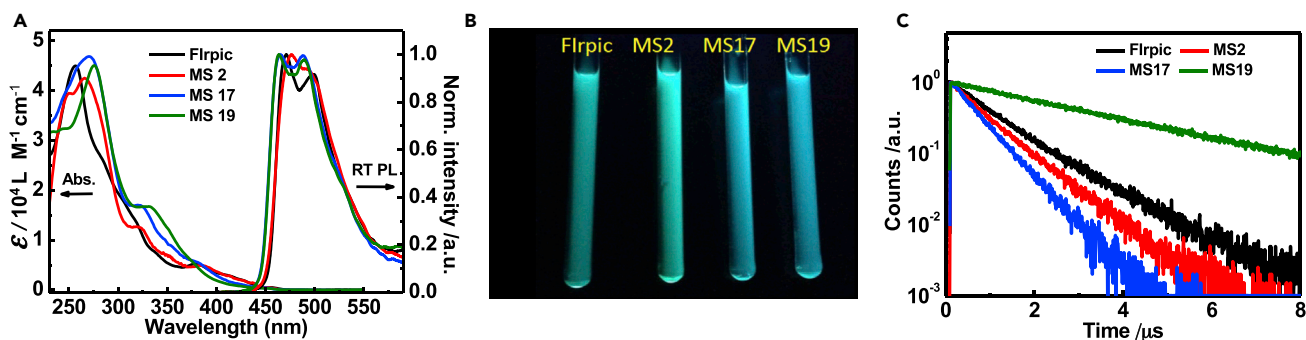


Figure 1. Photophysical Characteristics of Flrpic, MS 2, MS 17, and MS 19

(A) Absorption and PL spectra of the four Ir complexes in toluene at room temperature (10^{-5} M).

(B) Photo showing PL of Flrpic, MS 2, MS 17, and MS 19 (from left to right) in solution (in toluene under irradiation by a UV lamp at 365 nm).

(C) Transient PL decay curves of the four Ir complexes in toluene solution.

Also see Figure S1.

wavelength (versus Flrpic). The transient photoluminescence (PL) of **MS 2** shows a shorter phosphorescence lifetime ($0.82\ \mu\text{s}$) than that ($1.06\ \mu\text{s}$) of Flrpic, in agreement with the higher PLQY (0.88) of **MS 2** than that (0.85) of Flrpic observed in toluene solution. For practical utilization, the PL of **MS 2** doped (by 8 wt %) in a large triplet-energy host 9-(3-(9H-carbazol-9-yl)phenyl)-9H-carbazole-3-carbonitrile (mCPCN)³⁴ was also characterized (see *Supplemental Information* for the PL spectra in the mCPCN host). The emission spectrum is similar to that in solution, yet with a slightly higher (and nearly unitary) PLQY of 0.95 than that (0.93) of Flrpic (Table 1).

With physical properties and emission quantum yield promising for use as the emitting dopant in OLEDs, **MS 2** was subjected to EL study with the following device architecture (type I): indium tin oxide (ITO)/MoO₃ (1 nm)/1,1-bis[(di-4-tolylamino)phenyl]cyclohexane (TAPC; 40 nm)/N,N-dicarbazolyl-3,5-benzene (mCP; 10 nm)/mCPCN doped with 8 wt % of Ir complex (20 nm)/tris-[3-(3-pyridyl)mesityl]borane (3TPYMB; 50 nm)/LiF (1 nm)/Al (150 nm). Here, ITO and Al were used as the anode and cathode, respectively. TAPC and mCP were used as the hole-transport layers.³⁵ 3TPYMB was used as the electron-transport layer.³⁶ The bipolar mCPCN host doped with the efficient blue-emitting iridium dopants was used as the blue-emitting layer. MoO₃ and LiF were used as the hole and electron-injection layers.^{34,37} The high triplet energies of TAPC and 3TPYMB allow effective confinement of the generated triplet excitons within the emitting layer.³⁸ More details of device fabrication and characterization can be found in the *Supplemental Experimental Procedures* and Figure S2. Figure 2 depicts the EL characteristics of type I Flrpic and **MS 2** devices, and Table 2 summarizes the data. As in PL, relative to Flrpic, the **MS 2** device shows a slightly red-shifted 1931 CIE coordinate, whereas the benchmark Flrpic shows (0.160, 0.355) (Figure 2A). With the same device architecture, the devices based on both Flrpic and **MS 2** show very high maximum EL efficiency of up to (30.6%, $73.4\ \text{cd}\cdot\text{A}^{-1}$, $67.8\ \text{Im}\cdot\text{W}^{-1}$) and (30.1%, $79.4\ \text{cd}\cdot\text{A}^{-1}$, $69.3\ \text{Im}\cdot\text{W}^{-1}$), respectively, with relatively low turn-on voltage of $\sim 2.5\text{--}2.8\ \text{V}$ and low operation voltage (e.g., $\sim 3.5\ \text{V}$ for a brightness of $100\ \text{cd}\cdot\text{m}^{-2}$). Although **MS 2** and Flrpic could give similarly high peak EQEs, they exhibit quite different efficiency roll-off behaviors. The **MS 2** device retains a high EQE of $>25\%$ at the very high brightness of $8,000\ \text{cd}\cdot\text{m}^{-2}$. Meanwhile, the efficiency roll-off is more significant for the Flrpic device, for which the EQE drops to 17.2% at brightness of $8,000\ \text{cd}\cdot\text{m}^{-2}$. This result motivated us to further examine the device stability. The MoO₃ hole-injection layer of the type I device was replaced with 1,4,5,8,9,11-hexaaazatriphenylene hexacarbonitrile

Table 1. Physical and Photophysical Properties of the Iridium Complexes

Complex	λ_{abs} (nm) (ϵ [$\text{L mol}^{-1} \text{cm}^{-1}$]) ^a	E_g ^a (eV)	λ_{PL} ^a (nm)	ϕ_{PL} ^a (%)	τ ^a (μs)	ϕ_{film} ^b (%)	$\Theta_{ }$ ^b (%)	T_d ^c ($^{\circ}\text{C}$)	E_{ox} ^d (V)	E_{red} ^d (V)	HOMO/ LUMO ^e (eV)
Flrpic	455, 380 (4,500)	2.67	470	85	1.1	93	76	377	0.90	-2.6	-5.50/-2.83
	320 (14,300)		496							-2.2	
	255 (42,100)		498							-	
MS 2	456,386 (4,200)	2.64	475	88	0.8	95	77	339	1.10	-2.4	-5.70/-3.06
	323 (12,500)		499							-2.1	
	265 (43,100)		505							-	
MS 17	451,380 (4,500)	2.70	462	88	0.6	98	76	321	1.12	-2.4	-5.75/-3.05
	325 (17,600)		488							-2.1	
	270 (46,900)		475							-	
MS 19	452,375 (4,700)	2.69	463	86	3.3	97	75	264	1.13	-2.4	-5.76/-3.08
	333 (14,900)		499							-2.1	
	280 (44,300)		470							-	

^aUV-visible absorption peak and shoulder wavelengths λ_{abs} , molar extinction coefficient ϵ , the optical energy gap E_g determined from the absorption onset, PL peak and shoulder wavelengths λ_{PL} , PL quantum yield ϕ_{PL} , and excited-state lifetime τ measured in dilute (degassed) toluene solution (10^{-5} M) at room temperature.

^bPL quantum yield ϕ_{film} and horizontal dipole ratio $\Theta_{||}$ measured in the mCPCN-doped film at room temperature.

^c5% weight-loss temperatures T_d in TGA.

^dThe oxidation potential E_{ox} and reduction potentials E_{red} measured in acetonitrile.

^eHOMO levels calculated from oxidation potentials and LUMO levels obtained by $\text{HOMO}-E_g$.

(HATCN)³ to give a type II device for the investigation of device lifetime. The EL characteristics of the type II device incorporating Flrpic and MS 2 emitters are shown in Figure 3, and their EL performance parameters are summarized in Table 2. Although type II devices show slightly lower EL efficiencies than type I devices, they gave better operation durability. Figure 4 shows the relative decay of EL brightness as a function of the device operating time under a constant current driving (with a similar driving current density of $1.2\text{--}1.5 \text{ mA cm}^{-2}$) for type II devices. With a similar initial brightness of $330\text{--}350 \text{ cd}\cdot\text{m}^{-2}$, the device half-lifetimes (T_{50} , the time for the device brightness to decrease to 50% of its initial brightness) are 2.9 and 2,203 hr for type II Flrpic and MS 2 devices, respectively. Clearly, the MS 2-based device exhibits surprisingly long device operation lifetimes and durability, nearly three orders of magnitude longer than the typical benchmarking blue emitter Flrpic. The operation lifetime of $>2,200$ hr (at a brightness of $330\text{--}350 \text{ cd m}^{-2}$) is believed to be one of the best results for blue phosphorescent OLEDs (see Table 3 for comparison).^{39,41-45} Such an operation lifetime is generally one to two orders of magnitude longer than most of the lifetimes previously reported for blue phosphorescent OLEDs, as seen in Table 3. Moreover, the EQE of the long-lifetime device described here is also significantly higher than blue-emitting devices with reported lifetimes (Table 3).^{39,41-45} To date, the only comparable device lifetime results are perhaps those reported by Zhang et al.⁴² However, their device stability data were obtained from rather complicated graded doping and tandem device structures with lower EQEs. In comparison, our current work demonstrates a simple single-emitting unit, uniform doping device structure with both long lifespan and higher EL efficiencies. The results here thus suggest an intrinsic stability of the MS 2 complex and potentially even longer device lifetimes when adopting more robust and advanced device structures.

Despite its promising device efficiency and lifetime, the slightly red-shifted emission and thus poorer color purity of MS 2 could overshadow its practical application for display technology. Previous studies had manifested the fact that the N,N chelates

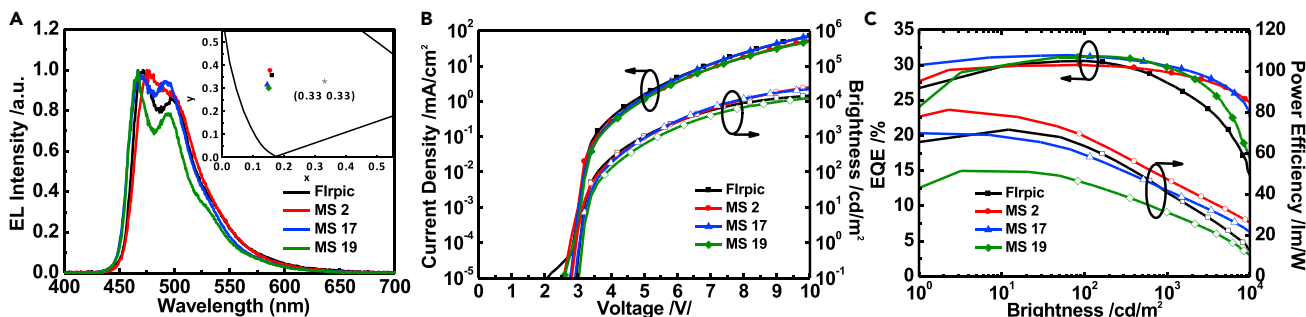


Figure 2. EL Characteristics of Type I Devices

EL spectra (A), current density-voltage-brightness (I-V-L) characteristics (B), and external quantum efficiency and power efficiency characteristics (C). Inset of (A) shows 1931 CIE (x , y) coordinates of various devices. 1931 CIE coordinates for Flrpic, MS 2, MS 17, and MS 19 devices are (0.160, 0.355), (0.154, 0.377), (0.145, 0.316), and (0.150, 0.301), respectively. Also see Figure S2.

such as 2-pyridyl-C-linked azolates are beneficial for attaining true-blue phosphors as a result of the increased ligand-centered π - π^* energy gaps.²⁷ Other groups have also demonstrated different design strategies and color tunability for blue phosphorescent Ir complexes, rendering decent device efficiencies.^{46–59} For instance, several studies have indicated that the emission properties of blue-emitting Ir complexes are harnessed not only by the cyclometalating ligands but also by the ancillary ligands.^{54–59} With the aim of obtaining bluer emission, we thus adopted strong-field ancillary CF_3 -containing pyridine-azole ligands, such as 2-(3-(trifluoromethyl)-1*H*-pyrazol-5-yl)pyridine³² and 2-(3,5-bis(trifluoromethyl)-1*H*-pyrrol-2-yl)pyridine,³³ to make the compounds MS 17 and MS 19 (Scheme 1), respectively. Incorporation of these ligands also gives us the chance to explore the impact of different ancillary ligands on the device stability. The syntheses and characterizations of these complexes are reported in Scheme S1. In addition to MS 2, the molecular structures of MS 17 and MS 19 have been resolved by single-crystal X-ray diffraction (XRD) analyses, as shown in Scheme 2 (also see Table S1 and Figure S3 for more details of the single-crystal XRD analyses). The complexes crystallize as distorted octahedrons where the ancillary ligands are found to display slightly longer Ir-N bonds than those of the cyclometalating ligands, i.e., Ir1–N1 (2.137(10) Å) versus Ir1–N2 (2.008(9) Å), Ir1–N4 (2.040(9) Å) in MS 2; Ir1–N2 (2.097(40) Å), Ir1–N3 (2.154(32) Å) versus Ir1–N4 (2.037(34) Å), Ir1–N6 (2.024(35) Å) in MS 17 and Ir1–N1 (2.132(43) Å), Ir1–N2 (2.133(49) Å) versus Ir1–N5 (2.043(40) Å), Ir1–N3 (2.029(43) Å) in MS 19. The result indicates that the anionic cyclometalated ligands have a stronger interaction with the Ir ion than the ancillary ligands. The dfppm cyclometalating ligands adopt a mutually eclipsed conformation with the N5 and N3 atoms being *trans* to each other. However, the overall structural arrangements in complexes MS 2, MS 17, and MS 19 resemble previously reported examples.^{60,61} The bite angles for the five-membered chelate rings of the cyclometalating ligands are found to be small and similar to Flrpic (80.7(160) $^\circ$, 81.5(185) $^\circ$), i.e., 80.4(424) $^\circ$, 80.5(436) $^\circ$ in MS 2; 80.4(138) $^\circ$, 80.2(134) $^\circ$ in MS 17; and 80.3(202) $^\circ$, 80.6(187) $^\circ$ in MS 19. Thus, these iridium complexes are expected to have similar ligand field states.

The thermal durability of pyrimidine-based Ir complexes (MS 2, MS 17, and MS 19) was investigated by thermogravimetric analysis (TGA) at a heating rate of 10°C per minute under an inert atmosphere. As summarized in Table 1, the 5% weight loss temperatures (T_d) were 339°C, 321°C, and 264°C for MS 2, MS 17, and MS 19, respectively (T_d of Flrpic, 377°C). The results indicate that these Ir complexes possess sufficient thermal stability for preparing thin films by high-vacuum thermal

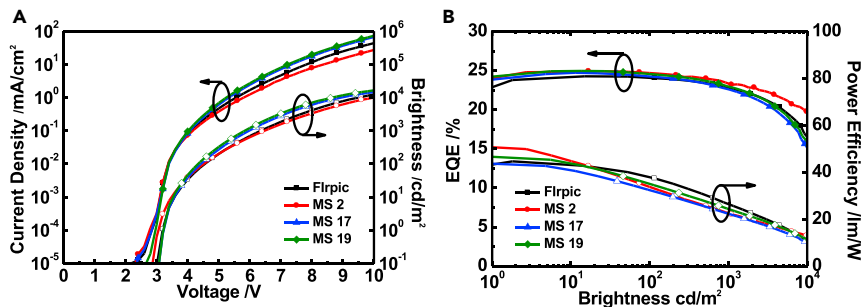
Table 2. Electroluminescence Characteristics of Type I and Type II OLEDs

Device		EQE (%)				η_p (lm W ⁻¹)				η_c (cd A ⁻¹)				CIE	
		max	100 cd m ⁻²	1,000 cd m ⁻²	8,000 cd m ⁻²	max	100 cd m ⁻²	1,000 cd m ⁻²	8,000 cd m ⁻²	max	100 cd m ⁻²	1,000 cd m ⁻²	8,000 cd m ⁻²	x	y
Type I	Flrpic	30.6	30.4	27.5	17.2	67.8	59.6	40.7	16.4	73.4	72.1	64.7	40.7	0.16	0.36
	MS 2	30.1	29.9	29.1	25.6	69.3	65.4	48.3	28.7	79.4	79.1	76.9	67.6	0.15	0.38
	MS 17	31.2	31.1	30	25.3	68.9	58.2	42.5	24.9	70.9	70.4	67.7	57.1	0.15	0.32
	MS 19	31.3	31.1	29.7	19.7	51.4	51.4	31.2	13.3	56.4	56.4	53.7	35.5	0.15	0.30
Type II	Flrpic	24.3	24	22.7	17.9	44.7	37.4	25.7	12.8	50.6	50.1	47.2	37.3	—	—
	MS 2	25	24.7	23.5	20.4	42.6	33.8	22.9	13.9	54.3	53.8	51.1	44.3	—	—
	MS 17	24.7	24.2	22.6	17.1	43.8	32.6	22.2	12	46.5	45.7	42.5	32.2	—	—
	MS 19	25	24.5	23	16.7	42.9	34.5	24.6	13.2	49.2	48.3	45.3	34.6	—	—

deposition. T_{d5} (5% weight loss) is dependent on different structural features of ancillary ligands, among which **MS 2** shows the highest temperature.

The electrochemical property of these Ir complexes was probed by cyclic voltammetry (Figure S4), and the data are summarized in Table 1. As the highest occupied molecular orbitals (HOMOs) of these complexes reside on the d orbitals of iridium and the π orbitals of the cyclometalating ligand, the well-resolved reversible oxidation peaks at 0.90 V, 1.10 V, 1.12 V, and 1.13 V for Flrpic, MS 2, MS 17, and MS 19, respectively, can be ascribed to oxidation of the iridium(III) metal center to iridium(IV) with a contribution from the cyclometalating ligands.^{62,63} Oxidation peaks shift positively by ≥ 200 mV in comparison with those of Flrpic, mainly as a result of the stronger electron-withdrawing nature of the pyrimidine moiety than of the pyridine moiety. Quasi-reversible reduction peaks were observed for all the complexes. With the lowest unoccupied molecular orbitals (LUMOs) mainly on the π^* orbitals of the cyclometalated ligands, the reduction occurs primarily on the pyridine rings for Flrpic, whereas it occurs mainly on the pyrimidine rings for the studied complexes. Thus, the first reduction potential of **MS 2**, **MS 17**, and **MS 19** is ~ 100 mV lower than that of Flrpic. Replacing pyridine with pyrimidine in cyclometalating ligands (e.g., Flrpic to **MS 2**) induces a slight decrease in the reduction potential. Further varying the ancillary ligand (from **MS 2** to **MS 17** and **MS 19**) does not bring any significant changes in reduction behavior. Based on the cyclic voltammetry (CV) results, the calculated HOMO/LUMO energy levels of Flrpic, **MS 2**, **MS 17**, and **MS 19** are summarized in Table 1.

Figure 5 shows the distributions of the HOMO and LUMO on optimized molecular geometries for compounds **MS 2**, **MS 17**, and **MS 19**, obtained with the time-dependent density function (TD-DFT) calculation; other computational details can be found in Tables S2 and S3–S5. The calculation predicts various geometric parameters, such as the Ir–ligand bond lengths and angles and the bite angles of the chelated rings, consistent with those obtained from XRD-resolved molecular structures. The calculation also confirms that the Ir–C bonds are shorter than the Ir–N bonds, agreeing well with the XRD-resolved structures and confirming that cyclometalating ligands bind more strongly to the metal center through the negatively charged carbon atom (versus the neutral nitrogen atom) (see Supplemental Information for details). As seen in Figure 5, HOMOs of **MS 2**, **MS 17**, and **MS 19** are mainly localized on the phenyl rings of the two cyclometalating ligands and the Ir center, although the contribution of the ancillary ligand to the HOMO is greater in **MS 19**. Meanwhile, the LUMOs have a π^* character delocalized on the phenyl and mostly

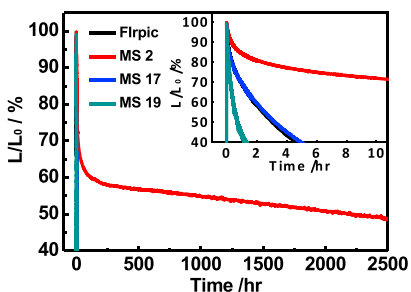
**Figure 3. EL Characteristics of Type II Devices**

- (A) Current-density-voltage-brightness (I-V-L) characteristics.
 (B) External quantum-efficiency and power-efficiency characteristics.

on the pyrimidine moieties of the two dfppm cyclometalating ligands, along with a minor contribution from the ancillary ligand. Theoretical calculations predict rather similar shifts in HOMO and LUMO energy levels ($-5.89/-2.07$, $-6.07/-2.24$, $-6.13/-2.21$, and $-6.19/-2.26$ eV for Flrpic, MS 2, MS 17, and MS 19, respectively), in agreement with the results obtained from CV.

The UV-visible spectra of these Ir complexes recorded in dilute toluene solutions show an intense band at ca. 260 nm and another band at ca. 320 nm, together with weaker bands from 350 to 450 nm (Figure 1). According to the calculations for various vertical excitation energies for these Ir complexes (see Figures S5 and S6), intense bands around 260 and 320 nm can be attributed to ligand-centered (LC) $^1(\pi-\pi^*)$ transitions on the cyclometalated ligands as well as the ancillary ligands, whereas weaker bands at 350–450 nm have charge-transfer character related to electronic transitions from the metal center to the ligands (spin-allowed $^1\text{MLCT}$), mixed with an intraligand/interligand charge-transfer transition ($^1\text{ILCT}/^1\text{LLCT}$). The extremely weak bands around 450 nm are attributed to an admixture of the spin-forbidden $^3\text{MLCT}$ and $^1\text{MLCT}$ transitions because of strong spin-orbit coupling of the heavy iridium atom.⁶⁴ The molar extinction coefficients (ϵ) were in the range 10,000–45,000 M⁻¹ cm⁻¹ for the ligand-centered $\pi-\pi^*$ bands and in the range of 4,000–5,000 M⁻¹ cm⁻¹ for the MLCT bands, as expected for iridium complexes.⁶⁵ Ir complexes with azole-based ancillary ligands (MS 17 and MS 19) generally show slightly higher molar extinction coefficients than complexes with picolinate-based ancillary ligands (Flrpic and MS 2). From the absorption edges at 463 and 464 nm for MS17 and MS 19, respectively, the corresponding optical energy gaps (E_g) were estimated to be 2.70 and 2.69 eV for MS17 and MS19, respectively, which are slightly larger than that of MS 2 (2.64 eV).

All four Ir complexes exhibit intense blue phosphorescence maximized at 460–475 nm with high PLQYs (ϕ_{PL}) in degassed toluene solution (Table 1). Replacement of the pyridine-based cyclometalating ligand with the pyrimidine-based cyclometalating ligand, but keeping the same picolinate-based ancillary ligand (i.e., from Flrpic to MS 2), results in a slight red shift (~5 nm) in emission peak wavelength (versus Flrpic). Further replacing the picolinate-based ancillary ligand with the azole-type ancillary ligand (i.e., MS 17 and MS 19), the stronger ligand field blue shifts the emission by ~12–14 nm (cf. Flrpic). These spectral shifts with varying different cyclometalating and ancillary ligands are consistent with the calculated trend for the Franck-Condon emission energies through the $\Delta\text{-SCF}$ method at the relaxed T₁ geometry (see *Supplemental Information*). The transient PL characteristics of the four Ir complexes in Figure 1 all show well-behaved mono-exponential

**Figure 4. OLED Device Lifetime**

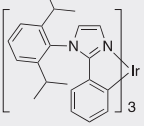
The decay of normalized EL brightness L (normalized to the initial brightness L_0) as a function of the device operating time under a constant current driving (with a similar driving current density of 1.5, 1.2, 1.4, and 1.3 mA cm^{-2} , corresponding to similar initial brightness of 339, 327, 351, and 329 cd m^{-2} , respectively) for four type II Flrpic, MS 2, MS 17, and MS 19 devices, respectively.

decay characteristics; extracted decay time constants and excited-state lifetimes τ are summarized in Table 1. Interestingly, MS 2 and MS 17 show shorter phosphorescence lifetimes (0.82 and 0.61 μs , respectively) than Flrpic (1.06 μs). The excited-state lifetimes of 0.6–0.8 μs are generally relatively short among efficient phosphorescent emitters and are beneficial for the OLED operation. In contrast, MS 19 possesses a significantly longer excited-state lifetime of 3.31 μs than the other three. Because these four Ir complexes possess similarly high PLQYs, such results indicate more effective (and faster) T_1 to S_0 radiative relaxation in MS 2 and MS 17 (versus Flrpic) and less effective T_1 to S_0 radiative relaxation in MS 19.

All these complexes show clear vibronic progression in their PL spectra. Previous literature on phosphorescent metal complexes suggest that emission dominated by metal-centered states are usually broad and featureless, whereas vibronic progressions often accompany emission associated with ligand-centered states.^{65–67} Thus, the observation of vibronic structure in PL indicates that the emissive excited states have ^3LC π - π^* character in addition to the $^3\text{MLCT}$ character.^{68–70} PL spectra of these Ir complexes (MS 2, MS 17, MS 19) show slight hypsochromic shift and spectral broadening when increasing the polarity of the solvent (see Figure S7), suggesting certain charge-transfer character (e.g., $^3\text{MLCT}/^3\text{ILCT}/^3\text{LLCT}$) of the emitting states. Indeed, such characteristics are well supported by the spin-density localization for the triplet (T_1) states of these Ir complexes determined by Mulliken spin-density analysis. From the unpaired electron spin density shown in Table S6 and Figure 5, it is evident that the emission in Ir complexes MS 2 and MS 17 can be assigned as the metal-to-ligand charge-transfer transition ($^3\text{MLCT}$) and the intraligand charge-transfer transition ($^3\text{ILCT}$) in the d_{ffppm} ligands. However, in the case of MS 19, the emission is composed of mixed $^3\text{MLCT}/^3\text{ILCT}/^3\text{LLCT}$ transitions because the unpaired electron spin density has a significant contribution from both the cyclometalating and ancillary ligands. The analysis carried out here is in good agreement with previous reports.^{71,72} The $^3\text{LLCT}$ possesses charge-transfer character and hence is relatively forbidden in transition in relation to that of $^3\text{ILCT}(\pi\pi^*)$. This leads to a significant difference between the excited-state lifetime of MS 19 and those of MS 2 and MS 17; the $T_1 \rightarrow S_1$ radiative lifetime of MS 19 is much longer than that of MS 2 or MS 17.

The PL of MS 17 and MS 19 doped (by 8 wt %) in mCPCN was also characterized (Figure S1). They show emission spectra similar to those in solutions yet with slightly higher (and nearly unitary) PLQYs for MS 17 (0.98) and MS 19 (0.97) than for Flrpic (0.93) and MS 2 (0.95) (Table 1). Furthermore, it has been recently reported that emitters with preferential horizontal (i.e., anisotropic) transition dipole orientation would benefit the optical out-coupling and improve the EQE of OLEDs.^{73–83} Considering the distinct asymmetric structures of these Ir(III) complexes, we characterized their emitting dipole orientations (in mCPCN host) by angle- and polarization-resolved

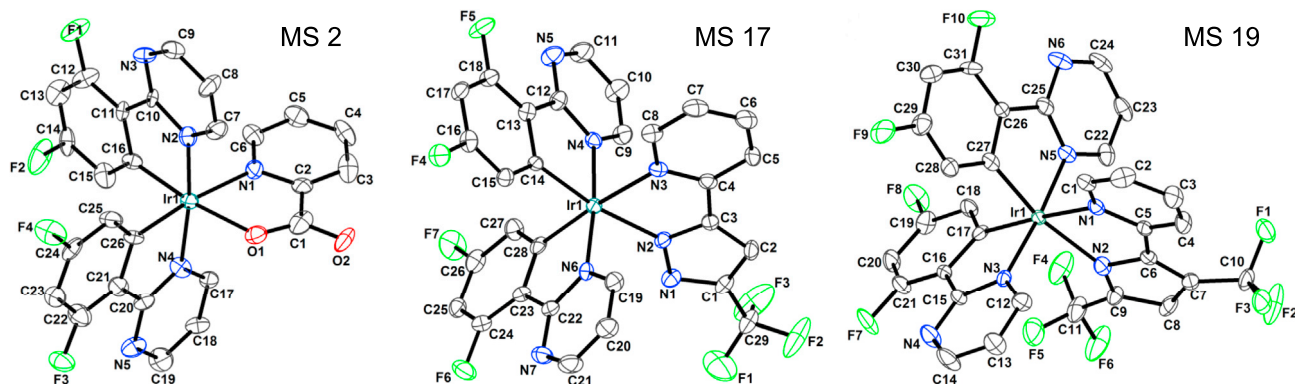
Table 3. Comparison of Reported Device Lifetimes for Blue Phosphorescent OLEDs

Host/Dopant	Peak EQE (%)	CIE	L_o^a (cd m $^{-2}$)	Lifetime b (hr)	Reference
mCPCN/MS 2	25 (54.3 cd A $^{-1}$)	0.16, 0.38	327	$T_{50} = 2,203$	this work c
CTPO/	(35.7 cd A $^{-1}$)	0.20, 0.38	1,000	$T_{50} = 5.2$	Zhuang et al. 39
					
mCBP/Ir(dfppy) $_2$ (pic-OH)	6.1	0.15, 0.35	400	$T_{50} = 34.3$	Yi et al. 40
mCBP/FIrpic	5.1	0.15, 0.36	400	$T_{50} = 20.1$	Yi et al. 40
BSB-CzSi/[Ir(mppm) $_2$ (pypz)]	12.5	0.14, 0.26	720	$T_{50} = 2.5$	Hsieh et al. 41
mCBP/Ir(dmp) $_3$	8.5	0.16, 0.31	1,000	$T_{50} = 510$	Zhang et al. 42
mCBP/Ir(dmp) $_3$ (graded doping)	9.5	0.16, 0.31	1,000	$T_{80} = 213$	Zhang et al. 42
mCBP/Ir(dmp) $_3$ (tandem device/graded doping)	18	0.15, 0.29	1,000	$T_{80} = 616$	Zhang et al. 42
mCBP/Ir(dbi) $_3$	14	0.19, 0.44	500	$T_{70} = 180$	Seo et al. 43
BCzDBT/Ir(dbi) $_3$	24.8	0.19, 0.41	1,000	$T_{50} = 140$	Yang and Lee 44
DBF-DMS/fac-Ir(iprprmi) $_3$	19.9	0.17, 0.40	1,000	$T_{50} = 122.6$	Zhang et al. 45

^aInitial brightness for the device stability test.^b T_{50} , T_{70} , and T_{80} represent the device lifetimes as the device brightness drops to 50%, 70%, and 80%, respectively, of the initial brightness L_o . For a fair comparison, the listed values are all experimentally measured values and not values estimated from extrapolation of experimental data via certain models.^cType II device data. Type I devices give higher efficiencies (i.e., 30.1%, 79.4 cd A $^{-1}$).

PL (see *Supplemental Experimental Procedures* for details). $^{73-83}$ Measured p-polarized PL intensities (at the PL peak wavelength) as a function of the emission angle for the four Ir complexes doped in mCPCN are shown in Figure 6. The measured curves are compared with simulated curves with different horizontal dipole ratios $\Theta_{||}$ (e.g., $\Theta_{||} = 100\%$ for fully horizontal dipoles and $\Theta_{||} = 67\%$ for the isotropic dipole orientation) to extract $\Theta_{||}$ values of different compounds in emitting layers. **MS 2**, **MS 17**, and **MS 19** all show preferential horizontal emitting dipole orientation with $\Theta_{||}$ values of 77%, 76%, and 75%, respectively (Table 1). These values are similar to $\Theta_{||}$ (76%) of FIrpic obtained here and in previous reports, 34,82,83 presumably because of their similar molecular structures and electronic transition mechanism among these phosphorescent complexes. $^{34,73-83}$ Consequently, with high (nearly unitary) PLQYs in combination with preferential horizontal dipole orientation in a thin-film host, **MS 2**, **MS 17**, and **MS 19** are promising for high-efficiency blue-emitting OLEDs.

The EL characteristics of type I devices incorporating **MS 17** and **MS 19** in the emitting layer are shown in Figures 2A–2C, and their EL performance parameters are summarized in Table 2. The EL spectra match well with the corresponding PL spectra of emitters in both solutions and doped films, indicating effective energy transfer from the host to the dopant. 1 The devices in general exhibit a relatively low turn-on voltage of ~ 2.5 – 2.8 V and low operation voltage (e.g., ~ 3.5 V for a brightness of 100 cd·m $^{-2}$). With the same device architecture, the devices based on **MS 17** and **MS 19** show higher EL efficiencies (up to 31.2% [70.9 cd·A $^{-1}$, 68.9 lm·W $^{-1}$] and 31.3% [56.4 cd·A $^{-1}$, 51.4 lm·W $^{-1}$], respectively) than FIrpic (30.6% [73.4 cd·A $^{-1}$, 67.8 lm·W $^{-1}$]) and **MS 2** (30.1% [79.4 cd·A $^{-1}$, 69.3 lm·W $^{-1}$]). With



Scheme 2. X-Ray Structures of MS 2, MS 17, and MS 19

The thermal ellipsoids are drawn at 50% probability, and the hydrogen atoms are omitted for clarity. Also see Table S1 and Figure S3.

similar maximal external quantum efficiencies, the variation of current efficiencies and power efficiencies among different emitters is mainly a result of their different EL colors (spectra). Importantly, EQEs of >31% from these devices are among the highest reported for blue phosphorescent OLEDs in conventional planar OLED structures that don't use any internal or external optical out-coupling schemes.⁸⁴ Such high EQEs are attributed to the high PLQYs of these emitters and their preferential horizontal dipole orientations.

Although these Ir(III) complexes could give similarly high peak EQEs, they exhibit quite different efficiency roll-off behaviors. **MS 2** and **MS 17** devices retain high EQEs of 29%–30% at the high brightness of 1,000 cd m⁻² and >25% even at the very high brightness of 8,000 cd m⁻². Meanwhile, the efficiency roll-off is more significant for **Flrpic** and **MS 19** devices, for which EQEs drop to 17.2% and 19.7%, respectively, at the high brightness of 8,000 cd m⁻². Such a trend in the efficiency roll-off appears to correlate well with their excited-state lifetimes τ (as listed in Table 1); **MS 2** and **MS 17** possess shorter excited-state lifetimes τ (0.6–0.8 μ s) than **Flrpic** and **MS 19** (1–3.3 μ s). A smaller τ indicates faster relaxation of emitting triplet excited states, beneficial for reducing the triplet exciton population at higher brightness/currents and thus for reducing associated quenching mechanisms (e.g., triplet-triplet annihilation, etc.).⁸⁵ The results and observations here thus suggest that the development of high-performance phosphorescent emitters should carefully consider τ values that are as short as possible, in addition to requiring high PLQYs and high horizontal dipole ratios.

The EL characteristics of type II devices incorporating **MS 17** and **MS 19** are shown in Figure 3, and their EL performance parameters are summarized in Table 2. Although type II devices show slightly lower EL efficiencies (with EQEs of up to 24.3%–25.8%) than type I devices, they generally give better operation durability. The device half-lifetimes T_{50} are 3.2 and 0.7 hr for type II **MS17** and **MS19** devices, respectively, which are comparable with that of the **Flrpic**-based device. Clearly, among the four blue-emitting Ir(III) complexes, **MS 2** exhibits the longest and most promising device operation lifetime and durability, nearly three orders of magnitude longer than the typical benchmarking blue emitter **Flrpic** as well as bluer emitters **MS 17** and **MS 19**. That the operation lifetime of the **MS 2** device outperforms that of other complexes, even with the same device structure, suggests its intrinsically better stability under the EL process in comparison with other complexes.

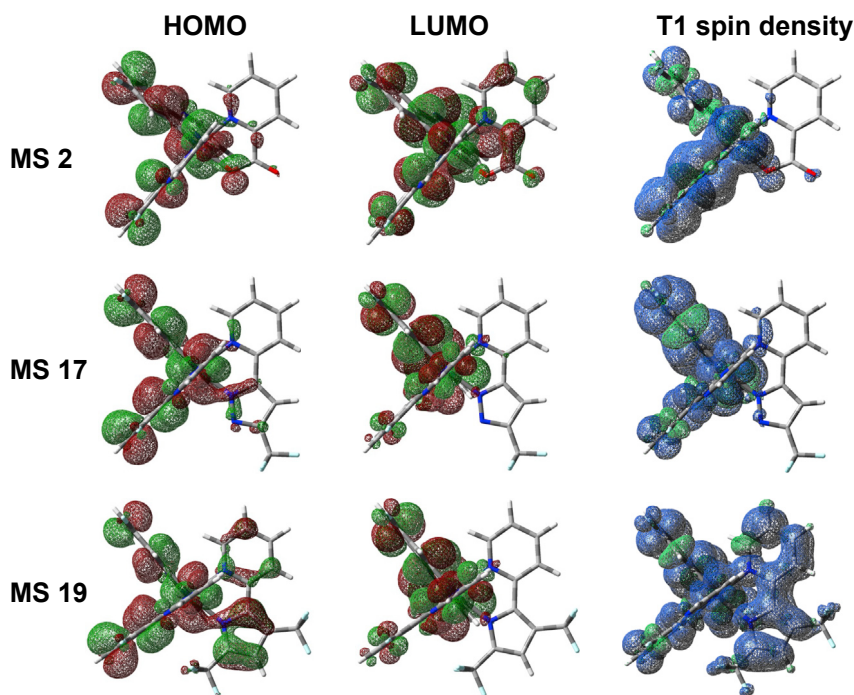


Figure 5. Theoretical Analysis of Molecular Orbitals

Spatial distributions of HOMOs and LUMOs for the optimized ground-state geometry of **MS 2**, **MS 17**, and **MS 19** and spin-density distribution calculated for the T_1 emitting excited state of **MS 2**, **MS 17**, and **MS 19**.

For rationalization, one of the lifetime-determining factors is ascribed to the ligand detachment in device operation. Upon pushing the Ir-based phosphorescent materials toward blue, it is inevitable that the emitting state energy increases toward the proximity of the metal-centered $d_{\pi}-d_{\sigma^*}$ state. Upon excitation, if the d-d state can be reached via thermal population, the metal-ligand bond becomes weakened, resulting in possible dissociation. We then carried out the computational approach to estimate the energy gap between metal center d-d transition, i.e., the 3MC state, and the emitting state (T_1 , 3MLCT) for these Ir complexes. The result shown in Figure S8 indicates that the relative energy between 3MC (metal center d-d transition) and 3MLCT states is rather small (<5 kcal mol⁻¹) for **MS 17** and **MS 19**. In sharp contrast, the 3MLCT - 3MC energy gap for **MS 2** and Flrpic is calculated to be ~15 and 12 kcal mol⁻¹, respectively. Because the calculated 3MC state energy is about the same for both **MS 2** and Flrpic, the difference in the energy gap lies in the lower 3MLCT state for **MS 2** because of its lower LUMO energy by inserting an additional nitrogen atom. As a result, under device operation, thermal activation from 3MLCT to 3MC states for Flrpic is more facile than for **MS 2**, resulting in population of the 3MC state that processes repulsive potential energy surface and hence the accessible channel for decomposition. The result rationalizes, in part, the superior stability of **MS 2** (cf. Flrpic) in terms of device stability.

Conclusion

In summary, we have revitalized research on phosphorescent Ir(III) complexes containing diazine-difluorophenyl-pyrimidine as the cyclometalating ligands, the potential of which has been largely underestimated because of their low EL efficiencies in previous preliminary studies. In this study, we conducted a comprehensive exploration on blue phosphorescent Ir(III) complexes with dfppy as the cyclometalating ligand and picolinate

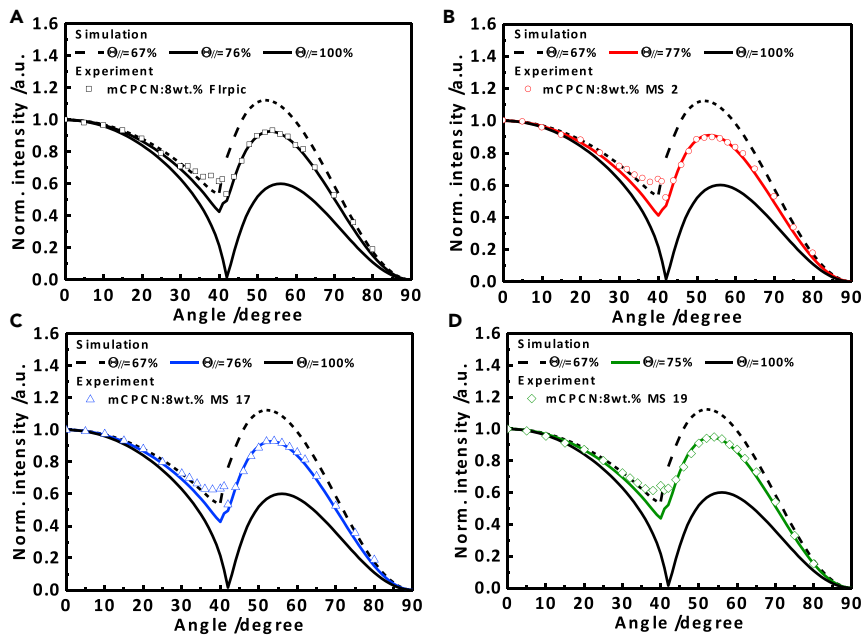


Figure 6. The Polarization of Photoluminescence

Measured (symbols) p-polarized PL intensity (at PL peak wavelength) of different emitting layers as a function of the emission angle: (A) mCPCN:8 wt % Flrpic, (B) mCPCN:8 wt % MS 2, (C) mCPCN:8 wt % MS 17, and (D) mCPCN:8 wt % MS 19. The measured curves are compared with simulated curves (lines) with different horizontal dipole ratios $\Theta_{||}$ (e.g., $\Theta_{||} = 100\%$ for fully horizontal dipoles and $\Theta_{||} = 67\%$ for the isotropic dipole orientation) for extraction of the horizontal emitting dipole ratios of different emitting layers.

or CF₃-substituted pyridine-azole as the ancillary ligand by benchmarking with the widely studied blue emitter Flrpic. Although simply replacing dfppy cyclometalating ligands in Flrpic (affording the compound MS 2) results in a slightly red-shifted emission, further replacing the picolinate-based ancillary ligand with strong-field CF₃-containing pyridine-azole ancillary ligands (affording compounds MS 17 and MS 19) offsets this red shift and leads to bluer emitters (versus Flrpic). As a result, these Ir(III) complexes yield omnibearing blue phosphorescent emitters with high PLQYs, preferential horizontal emitting dipole orientations, short excited lifetimes, high EL efficiencies (EQE > 31%), low efficiency roll-off, and promising device operation durability ($T_{50} \sim 2,203$ hr for MS 2) ready for practical application.

EXPERIMENTAL PROCEDURES

Synthesis

The syntheses of title Ir complexes were followed reported procedure (also see Scheme S1). For the detail synthetic procedures and characterizations, please see the [Supplemental Experimental Procedures](#).

Determination of Emitting Dipole Orientation

To determine the emitting dipole orientation in a molecular emitting film, angle-resolved and polarization-resolved PL measurements were performed. The sample consisted of a glass substrate with a 20-nm-thick mCPCN film doped with emitters. The sample was attached to a fused silica half cylinder prism by index matching liquid. The excitation of the samples was performed with the 325-nm line of a continuous-wave He:Cd laser with a fixed excitation angle of 45°. The emission angle was changed using a rotating stage. The spectra were measured with a fiberoptic

spectrometer and a polarizing filter to distinguish p- and s-polarized light. The angle-dependent p-polarized emission intensity at the peak wavelength of the PL spectrum of the emitting layer was detected. The emitting dipole orientation (the horizontal dipole ratio $\Theta_{||}$) was then determined by comparing the measured angle-dependent p-polarized emission intensity with those calculated assuming different horizontal dipole ratios ($\Theta_{||}$).

ACCESSION NUMBERS

Crystal data for **MS 2**, **MS 17**, and **MS 19** have been deposited in the Cambridge Crystallographic Data Center under CCDC: 1553498, 1553499, and 1553500, respectively.

SUPPLEMENTAL INFORMATION

Supplemental Information includes Supplemental Experimental Procedures, eight figures, one scheme, and six tables and can be found with this article online at <http://dx.doi.org/10.1016/j.chempr.2017.08.001>.

AUTHOR CONTRIBUTIONS

M.S. synthesized the Ir complexes and characterized their structures and properties. Y.C. synthesized and provided intermediate reagents for the syntheses of Ir complexes. W.-L.T. fabricated and characterized the devices. W.-K.L. measured the spectra of the thin films, excited-state lifetimes of the solutions and films, and emitting dipole orientations in the thin films. M.S., W.-L.T., and W.-K.L. also helped prepare the manuscript. M.S. and S.-H.L. performed the theoretical analyses. P.-T.C., C.-C.W., and K.-T.W. supervised the project and wrote the manuscript. All authors discussed the results.

ACKNOWLEDGMENTS

The authors gratefully acknowledge financial support from the Ministry of Science and Technology of Taiwan (MOST 104-2113-M-002-006-MY3 and 104-2221-E-002-152-MY3).

Received: March 21, 2017

Revised: June 5, 2017

Accepted: August 3, 2017

Published: September 14, 2017

REFERENCES

1. Cui, L.S., Liu, Y., Liu, X.-Y., Jiang, Z.-Q., and Liao, L.-S. (2015). Design and synthesis of pyrimidine-based iridium(III) complexes with horizontal orientation for orange and white phosphorescent OLEDs. *ACS Appl. Mater. Inter.* 7, 11007–11014.
2. Reineke, S., Lindner, F., Schwartz, G., Seidler, N., Walzer, K., Lüssem, B., and Leo, K. (2009). White organic light-emitting diodes with fluorescent tube efficiency. *Nature* 459, 234–238.
3. Liao, L.S., Slusarek, W.K., Hatwar, T.K., Ricks, M.L., and Comfort, D.L. (2008). Tandem organic light-emitting diode using hexaazatriphenylene hexacarbonitrile in the intermediate connector. *Adv. Mater.* 20, 324–329.
4. Wang, Q., Ding, J., Ma, D., Cheng, Y., Wang, L., Jing, X., and Wang, F. (2009). Harvesting excitons via two parallel channels for efficient white organic LEDs with nearly 100% internal quantum efficiency: fabrication and emission-mechanism analysis. *Adv. Funct. Mater.* 19, 84–95.
5. Adachi, C., Baldo, M.A., Thompson, M.E., and Forrest, S.R. (2001). Nearly 100% internal phosphorescence efficiency in an organic light-emitting device. *J. Appl. Phys.* 90, 5048–5051.
6. Ikai, M., Tokito, S., Sakamoto, Y., Suzuki, T., and Taga, Y. (2001). Highly efficient phosphorescence from organic light-emitting devices with an exciton-block layer. *Appl. Phys. Lett.* 79, 156–158.
7. Sasabe, H., and Kido, J. (2013). Development of high performance OLEDs for general lighting. *J. Mater. Chem. C* 1, 1699–1707.
8. Sasabe, H., and Kido, J. (2013). Recent progress in phosphorescent organic light-emitting devices. *Eur. J. Org. Chem.* 2013, 7653–7663.
9. Ye, H., Liu, C.-M., Su, S.-J., Wang, Y.-F., Lo, C.-C., Lien, A., and Kido, J. (2014). Pyridine-containing electron-transport materials for highly efficient blue phosphorescent OLEDs with ultralow operating voltage and reduced efficiency roll-off. *Adv. Funct. Mater.* 24, 3268–3275.
10. Duan, T., Chang, T.-K., Chi, Y., Wang, J.-Y., Chen, Z.-N., Hung, W.-Y., Chen, C.-H., and Lee, G.-H. (2015). Blue-emitting heteroleptic Ir(III) phosphors with functional 2,3'-bipyridine or 2-(pyrimidin-5-yl)pyridine cyclometalates. *Dalton Trans.* 44, 14613–14624.
11. Wang, R., Liu, D., Ren, H., Zhang, T., Yin, H., Liu, G., and Li, J. (2011). Highly efficient orange and

- white organic light-emitting diodes based on new orange iridium complexes. *Adv. Mater.* 23, 2823–2827.
12. Fan, C., Li, Y., Yang, C., Wu, H., Qin, J., and Cao, Y. (2012). Phosphoryl/sulfonyl-substituted iridium complexes as blue phosphorescent emitters for single-layer blue and white organic light-emitting diodes by solution process. *Chem. Mater.* 24, 4581–4587.
13. Chou, H.H., Li, Y.K., Chen, Y.H., Chang, C.C., Liao, C.Y., and Cheng, C.H. (2013). New iridium dopants for white phosphorescent devices: enhancement of efficiency and color stability by an energy-harvesting layer. *ACS Appl. Mater. Inter.* 5, 6168–6175.
14. Jou, J.H., Lin, Y.X., Peng, S.H., Li, C.J., Yang, Y.M., Chin, C.L., and Hu, J.P. (2014). Highly efficient yellow organic light emitting diode with a novel wet- and dry-process feasible iridium complex emitter. *Adv. Funct. Mater.* 24, 555–562.
15. Li, G., Zhu, D., Peng, T., Liu, Y., Wang, Y., and Bryce, M.R. (2014). Very high efficiency orange-red light-emitting devices with low roll-off at high luminance based on an ideal host–guest system consisting of two novel phosphorescent iridium complexes with bipolar transport. *Adv. Funct. Mater.* 24, 7420–7426.
16. Cao, H., Shan, G., Wen, X., Sun, H., Su, Z., Zhong, R., and Zhu, D. (2013). An orange iridium(III) complex with wide-bandwidth in electroluminescence for fabrication of high-quality white organic light-emitting diodes. *J. Mater. Chem. C* 1, 7371–7379.
17. Li, T.-Y., Liang, X., Zhou, L., Wu, C., Zhang, S., Liu, X., Lu, G.-Z., Xue, L.-S., Zheng, Y.-X., and Zuo, J.-L. (2015). N-heterocyclic carbenes: versatile second cyclometalated ligands for neutral iridium(III) heteroleptic complexes. *Inorg. Chem.* 54, 161–173.
18. Adachi, C., Kwong, R.C., Djurovich, P., Adamovich, V., Baldo, M.A., Thompson, M.E., and Forrest, S.R. (2001). Endothermic energy transfer: a mechanism for generating very efficient high-energy phosphorescent emission in organic materials. *Appl. Phys. Lett.* 79, 2082–2084.
19. Ahn, S.Y., and Ha, Y. (2009). The blue phosphorescent iridium complexes containing new triazole ligands for OLEDs. *Mol. Cryst. Liq. Cryst.* 504, 59–66.
20. Sajoto, T., Djurovich, P.I., Tamayo, A.B., Osgaard, J., Goddard, W.A., III, and Thompson, M.E. (2009). Temperature dependence of blue phosphorescent cyclometalated Ir(III) complexes. *J. Am. Chem. Soc.* 131, 9813–9822.
21. Rausch, A.F., Thompson, M.E., and Yersin, H. (2009). Matrix effects on the triplet state of the OLED emitter $\text{Ir}(4,6\text{-dFppy})_2(\text{pic})$ (Flpic): investigations by high-resolution optical spectroscopy. *Inorg. Chem.* 48, 1928–1937.
22. Park, H.R., Lim, D.H., Kim, Y.K., and Ha, Y. (2012). The new iridium complexes involving pyridylpyridine derivatives for the saturated blue emission. *J. Nanosci. Nanotechnol.* 12, 668–673.
23. Wu, Z.-G., Jing, Y.-M., Lu, G.-Z., Zhou, J., Zheng, Y.-X., Zhou, L., Wang, Y., and Pan, Y. (2016). Novel design of iridium phosphors with pyridinylphosphinate ligands for high-efficiency blue organic light-emitting diodes. *Sci. Rep.* 6, 38478.
24. Yeh, S.-J., Wu, M.-F., Chen, C.-T., Song, Y.-H., Chi, Y., Ho, M.-H., Hsu, S.-F., and Chen, C.H. (2005). New dopant and host materials for blue-light-emitting phosphorescent organic electroluminescent devices. *Adv. Mater.* 17, 285–289.
25. Yang, C.-H., Cheng, Y.-M., Chi, Y., Hsu, C.-J., Fang, F.-C., Wong, K.-T., Chou, P.-T., Chang, C.-H., Tsai, M.-H., and Wu, C.-C. (2007). Blue-emitting heteroleptic iridium(III) complexes suitable for high-efficiency phosphorescent OLEDs. *Angew. Chem. Int. Ed.* 46, 2418–2421.
26. Yang, C.-H., Li, S.-W., and Chi, Y. (2005). Heteroleptic cyclometalated iridium(III) complexes displaying blue phosphorescence in solution and solid state at room temperature. *Inorg. Chem.* 44, 7770–7780.
27. Chi, Y., and Chou, P.-T. (2010). Transition-metal phosphors with cyclometalating ligands: fundamentals and applications. *Chem. Soc. Rev.* 39, 638–655.
28. Jurow, M.J., Mayr, C., Schmidt, T.D., Lampe, T., Djurovich, P.I., Brüttig, W., and Thompson, M.E. (2016). Understanding and predicting the orientation of heteroleptic phosphors in organic light-emitting materials. *Nature* 515, 85–91.
29. Ge, G., Yu, X., Guo, H., Wang, F., and Zou, D. (2009). Polymer-based blue electrophosphorescent light-emitting diodes based on a new iridium(III) diazine complex. *Synth. Met.* 159, 1178–1182.
30. Ge, G., He, J., Guo, H., Wang, F., and Zou, D. (2009). Highly efficient phosphorescent iridium(III) diazine complexes for OLEDs: different photophysical property between iridium(III) pyrazine complex and iridium(III) pyrimidine complex. *J. Organomet. Chem.* 694, 3050–3057.
31. Chen, H.-F., Chi, L.-C., Hung, W.-Y., Chen, W.-J., Hwu, T.-Y., Chen, Y.-H., Chou, S.-H., Mondal, E., Liu, Y.-H., and Wong, K.-T. (2012). Carbazole and benzimidazole/oxadiazole hybrids as bipolar host materials for sky blue, green, and red PhOLEDs. *Org. Electron.* 13, 2671–2681.
32. Thiel, W.R., and Eppinger, J. (1997). Molybdenum-catalyzed olefin epoxidation: ligand effects. *Chem. Eur. J.* 3, 696–705.
33. Ohkura, H., Berbasov, D.O., and Soloshonok, V.A. (2003). Simple and highly diastereoselective synthesis of trifluoromethyl-containing myosamines via reaction between 2-(aminomethyl)pyridine and 1,1,1,5,5-hexafluoro-2,4-pentanedione. *Tetrahedron Lett.* 44, 2417–2420.
34. Lin, M.-S., Yang, S.-J., Chang, H.-W., Huang, Y.-H., Tsai, Y.-T., Wu, C.-C., Chou, S.-H., Mondal, E., and Wong, K.-T. (2012). Incorporation of a CN group into mCP: a new bipolar host material for highly efficient blue and white electrophosphorescent devices. *J. Mater. Chem.* 22, 16114–16120.
35. Xiao, L., Su, S.J., Agata, Y., Lan, H., and Kido, J. (2009). Nearly 100% internal quantum efficiency in an organic blue-light electrophosphorescent device using a weak electron transporting material with a wide energy gap. *Adv. Mater.* 21, 1271–1274.
36. Tanaka, D., Takeda, T., Chiba, T., Watanabe, S., and Kido, J. (2007). Novel electron-transport material containing boron atom with a high triplet excited energy level. *Chem. Lett.* 36, 262–263.
37. Wu, C.-C., Lin, Y.-T., Wong, K.-T., Chen, R.-T., and Chien, Y.-Y. (2004). Efficient organic blue-light-emitting devices with double confinement on terphenoles with ambipolar carrier transport properties. *Adv. Mater.* 16, 61–65.
38. Liu, D., Ren, H., Deng, L., and Zhang, T. (2013). Synthesis and electrophosphorescence of iridium complexes containing benzothiazole-based ligands. *ACS Appl. Mater. Inter.* 5, 4937–4944.
39. Zhuang, J., Li, W., Wu, W., Song, M., Su, W., Zhou, M., and Cui, Z. (2015). Homoleptic tris-cyclometalated iridium(III) complexes with phenylimidazole ligands for highly efficient sky-blue OLEDs. *New J. Chem.* 39, 246–253.
40. Yi, S., Kim, J.-H., Cho, Y.-J., Lee, J., Choi, T.-S., Cho, D.W., Pac, C., Han, W.-S., Son, H.-J., and Kang, S.O. (2016). Stable blue phosphorescence iridium(III) cyclometalated complexes prompted by intramolecular hydrogen bond in ancillary ligand. *Inorg. Chem.* 55, 3324–3331.
41. Hsieh, C.-H., Wu, F.-I., Fan, C.-H., Huang, M.-J., Lu, K.-Y., Chou, P.-Y., Yang, Y.-H.O., Wu, S.-H., Chen, I.-C., Chou, S.-H., et al. (2011). Design and synthesis of iridium bis(carbene) complexes for efficient blue electrophosphorescence. *Chem. Eur. J.* 17, 9180–9187.
42. Zhang, Y., Lee, J., and Forrest, S.R. (2014). Tenfold increase in the lifetime of blue phosphorescent organic light-emitting diodes. *Nat. Commun.* 5, 5008.
43. Seo, J.-A., Jeon, S.K., Gong, M.S., Lee, J.Y., Noh, C.H., and Kim, S.H. (2015). Long lifetime blue phosphorescent organic light-emitting diodes with an exciton blocking layer. *J. Mater. Chem. C* 3, 4640–4645.
44. Yang, J.W., and Lee, J.Y. (2015). Correlation of the molecular structure of host materials with lifetime and efficiency of blue phosphorescent organic light-emitting diodes. *Phys. Chem. Chem. Phys.* 17, 24468–24474.
45. Zhang, L., Zhang, Y.-X., Hu, Y., Shi, X.-B., Jiang, Z.-Q., Wang, Z.-K., and Liao, L.-S. (2016). Highly efficient blue phosphorescent organic light-emitting diodes employing a host material with small bandgap. *ACS Appl. Mater. Inter.* 8, 16186–16191.
46. Yun, S.-J., Seo, H.-J., Song, M., Jin, S.-H., and Kim, Y.I. (2012). Blue emitting cationic iridium complexes containing two substituted 2-phenylpyridine and one 2,2'-biimidazole for solution-processed organic light-emitting diodes (OLEDs). *Bull. Korean Chem. Soc.* 33, 3645–3650.
47. Thamilarasan, V., Jayamani, A., Manisankar, P., Kim, Y.-I., and Sengottuvelan, N. (2013). Green-emitting phosphorescent iridium (III) complex: structural, photophysical and electrochemical properties. *Inorg. Chim. Acta* 408, 240–245.

48. Yun, S.-J., Seo, H.-J., Song, M., Jin, S.-H., Kang, S.K., and Kim, Y.-I. (2013). Sky-blue phosphorescent iridium(III) complexes with two substituted 2-phenylpyridine derivatives and one picolinic acid for organic light-emitting diodes. *J. Organomet. Chem.* 724, 244–250.
49. Lee, S.-J., Park, J.-S., Song, M., Shin, I.A., Kim, Y.-I., Lee, J.W., Kang, J.-W., Gal, Y.-S., Kang, S., Lee, J.Y., et al. (2009). Synthesis and characterization of red-emitting iridium(III) complexes for solution-processable phosphorescent organic light-emitting diodes. *Adv. Funct. Mater.* 19, 2205–2212.
50. Wang, C.-C., Jing, Y.-M., Li, T.-Y., Xu, Q.-L., Zhang, S., Li, W.-N., Zheng, Y.-X., Zuo, J.-L., You, X.-Z., and Wang, X.-Q. (2013). Syntheses, photoluminescence, and electroluminescence of iridium(III) complexes with fluorinated 2-phenylpyridine as main ligands and tetraphenylimidodiphosphinate as ancillary ligand. *Eur. J. Inorg. Chem.* 2013, 5683–5693.
51. Orsell, E., Kottas, G.S., Konradsson, A.E., Coppo, P., Fröhlich, R., De Cola, L., Dijken, A.V., Büchel, M., and Börner, H. (2007). Blue-emitting iridium complexes with substituted 1,2,4-triazole ligands: synthesis, photophysics, and devices. *Inorg. Chem.* 46, 11082–11093.
52. Su, H.-C., Chen, H.-F., Fang, F.-C., Liu, C.-C., Wu, C.-C., Wong, K.-T., Liu, Y.-H., and Peng, S.-M. (2008). Solid-state white light-emitting electrochemical cells using iridium-based cationic transition metal complexes. *J. Am. Chem. Soc.* 130, 3413–3419.
53. Klubek, K.P., Dong, S.-C., Liao, L.-S., Tang, C.W., and Rothberg, L.J. (2014). Investigating blue phosphorescent iridium cyclometalated dopant with phenyl-imidazole ligands. *Org. Electron.* 15, 3127–3136.
54. Kessler, F., Watanabe, Y., Sasabe, H., Katagiri, H., Nazeeruddin, M.K., Grätzel, M., and Kido, J. (2013). High-performance pure blue phosphorescent OLED using a novel bis-heteroleptic iridium(III) complex with fluorinated bipyridyl ligands. *J. Mater. Chem. C* 1, 1070–1075.
55. Udagawa, K., Sasabe, H., Cai, C., and Kido, J. (2014). Low-driving-voltage blue phosphorescent organic light-emitting devices with external quantum efficiency of 30%. *Adv. Mater.* 26, 5062–5066.
56. Sasabe, H., Nakanishi, H., Watanabe, Y., Yano, S., Hirasawa, M., Pu, Y.-J., and Kido, J. (2013). Extremely low operating voltage green phosphorescent organic light-emitting devices. *Adv. Funct. Mater.* 23, 5550–5555.
57. Monti, F., Kessler, F., Delgado, M., Frey, J., Bazzanini, F., Accorsi, G., Armarni, N., Bolink, H.J., Ortí, E., Scopelliti, R., et al. (2013). Charged bis-cyclometalated iridium(III) complexes with carbene-based ancillary ligands. *Inorg. Chem.* 52, 10292–10305.
58. Baranoff, E., and Curchod, B.F.E. (2015). Flrpic: archetypal blue phosphorescent emitter for electroluminescence. *Dalton Trans.* 44, 8318–8329.
59. Kim, K.-H., Lee, S., Moon, C.-K., Kim, S.-Y., Park, Y.-S., Lee, J.-H., Lee, J.W., Huh, J., You, Y., and Kim, J.-J. (2014). Phosphorescent dye-based supramolecules for high-efficiency organic light-emitting diodes. *Nature* 5, 4769.
60. Lee, S.-J., Park, K.-M., Yang, K., and Kang, Y. (2009). Blue phosphorescent Ir(III) complex with high color purity: fac-Tris(2',6'-difluoro-2,3'-bipyridinato-N,C')²⁺iridium(III). *Inorg. Chem.* 48, 1030–1037.
61. Yang, C.-H., Mauro, M., Polo, F., Watanabe, S., Muenster, I., Fröhlich, R., and De Cola, L. (2012). Deep-blue-emitting heteroleptic iridium(III) complexes suited for highly efficient phosphorescent OLEDs. *Chem. Mater.* 24, 3684–3695.
62. Hasan, K., Pal, A.K., Auvray, T., Zysman-Colman, E., and Hanan, G.S. (2015). Blue-green emissive cationic iridium(III) complexes using partially saturated strongly-donating guanidyl-pyridine-/pyrazine ancillary ligands. *Chem. Commun.* 51, 14060–14063.
63. Fernández-Hernández, J.M., Beltrán, J.I., Lemaur, V., Gálvez-López, M.-D., Chien, C.-H., Polo, F., Orsell, E., Fröhlich, R., Cornil, J., and De Cola, L. (2013). Iridium(III) emitters based on 1,4-disubstituted-1H-1,2,3-triazoles as cyclometalated ligand: synthesis, characterization, and electroluminescent devices. *Inorg. Chem.* 52, 1812–1824.
64. Sunesh, C.D., Shanmugasundaram, K., Subeesh, M.S., Chitumalla, R.K., Jang, J., and Choe, Y. (2015). Blue and blue-green light-emitting cationic iridium complexes: synthesis, characterization, and optoelectronic properties. *ACS Appl. Mater. Inter.* 7, 7741–7751.
65. Lamansky, S., Djurovich, P., Murphy, D., -Razzaq, F.A., Lee, H.-E., Adachi, C., Burrows, P.E., Forrest, S.R., and Thompson, M.E. (2001). Highly phosphorescent bis-cyclometalated iridium complexes: synthesis, photophysical characterization, and use in organic light emitting diodes. *J. Am. Chem. Soc.* 123, 4304–4312.
66. Spellane, P., Watts, R.J., and Vogler, A. (1993). Luminescence characterizations of cyclometalated rhodium(I) carbonyl complexes. *Inorg. Chem.* 32, 5633–5636.
67. Sarma, M., Chatterjee, T., Bodapati, R., Krishnanth, K.N., Hamad, S., Venugopal Rao, S., and Das, S.K. (2016). Cyclometalated iridium(III) complexes containing 4,4'- π -conjugated 2,2'-bipyridine derivatives as the ancillary ligands: synthesis, photophysics, and computational studies. *Inorg. Chem.* 55, 3530–3540.
68. Tamayo, A.B., Garon, S., Sajoto, T., Djurovich, P.I., Tsby, I.M., Bau, R., and Thompson, M.E. (2005). Cationic bis-cyclometalated iridium(III) diimine complexes and their use in efficient blue, green, and red electroluminescent devices. *Inorg. Chem.* 44, 8723–8732.
69. Sprouse, S., King, K.A., Spellane, P.J., and Watts, R.J. (1984). Photophysical effects of metal-carbon. σ . bonds in ortho-metallated complexes of iridium(III) and rhodium(III). *J. Am. Chem. Soc.* 106, 6647–6653.
70. Tsuboyama, A., Iwawaki, H., Furugori, M., Mukaiide, T., Kamatani, J., Igawa, S., Moriyama, T., Miura, S., Takiguchi, T., Okada, S., et al. (2003). Homoleptic cyclometalated iridium complexes with highly efficient red phosphorescence and application to organic light-emitting diode. *J. Am. Chem. Soc.* 125, 12971–12979.
71. Welby, C.E., Gilmartin, L., Marriott, R.R., Zahid, A., Rice, C.R., Gibson, E.A., and Elliott, P.I.P. (2013). Luminescent biscyclometalated arylpyridine iridium(III) complexes with 4,4'-bi-1,2,3-triazolyl ancillary ligands. *Dalton Trans.* 42, 13527–13536.
72. Qu, X., Liu, Y., Si, Y., Wu, X., and Wu, Z. (2014). A theoretical study on supramolecularly-caged positively charged iridium(III) 2-pyridyl azolate derivatives as blue emitters for light-emitting electrochemical cells. *Dalton Trans.* 43, 1246–1260.
73. Ho, P.K.H., Kim, J.-S., Burroughes, J.H., Becker, H., Li, S.F.Y., Brown, T.M., Caciulli, F., and Friend, R.H. (2000). Molecular-scale interface engineering for polymer light-emitting diodes. *Nature* 404, 481–484.
74. Smith, L.H., Wasey, J.A.E., Samuel, I.D.W., and Barnes, W.L. (2005). Light out-coupling efficiencies of organic light-emitting diode structures and the effect of photoluminescence quantum yield. *Adv. Funct. Mater.* 15, 1839–1844.
75. Flämmich, M., Gather, M.C., Danz, N., Michaelis, D., Brauer, A.H., Meerholz, K., and Tunnermann, A. (2010). Orientation of emissive dipoles in OLEDs: quantitative *in situ* analysis. *Org. Electron.* 11, 1039–1046.
76. Lin, H.-W., Lin, C.-L., Chag, H.-H., Lin, Y.-T., Wu, C.-C., Chen, Y.-M., Chen, R.-T., Chien, Y.-Y., and Wong, K.-T. (2004). Anisotropic optical properties and molecular orientation in vacuum-deposited ter(9,9-diarylfluorene)s thin films using spectroscopic ellipsometry. *J. Appl. Phys.* 95, 881–886.
77. Lin, H.-W., Lin, C.-L., Wu, C.-C., Chao, T.-C., and Wong, K.-T. (2007). Influences of molecular orientations on stimulated emission characteristics of oligofluorene films. *Org. Electron.* 8, 189–197.
78. Yokoyama, D., Sasabe, H., Furukawa, Y., Adachi, C., and Kido, J. (2011). Molecular stacking induced by intermolecular C–H...N hydrogen bonds leading to high carrier mobility in vacuum-deposited organic films. *Adv. Funct. Mater.* 21, 1375–1382.
79. Frischeisen, J., Yokoyama, D., Endo, A., Adachi, C., and Brüttling, W. (2011). Increased light outcoupling efficiency in dye-doped small molecule organic light-emitting diodes with horizontally oriented emitters. *Org. Electron.* 12, 809–817.
80. Schmidt, T.D., Setz, D.S., Flämmich, M., Frischeisen, J., Michaelis, D., Krummacher, B.C., Danz, N., and Brüttling, W. (2011). Evidence for non-isotropic emitter orientation in a red phosphorescent organic light-emitting diode and its implications for determining the emitter's radiative quantum efficiency. *Appl. Phys. Lett.* 99, 163302.
81. Penninck, L., Steinbacher, F., Krause, R., and Neyts, K. (2012). Determining emissive dipole orientation in organic light emitting devices by decay time measurement. *Org. Electron.* 13, 3079–3084.
82. Liehm, P., Murawski, C., Furno, M., Lüssem, B., Leo, K., and Gather, M.C. (2012).

- Measurement of threshold voltage in organic thin film transistors. *Appl. Phys. Lett.* 25, 253304.
83. Kim, S.-Y., Jeong, W.-I., Mayr, C., Park, Y.-S., Kim, K.-H., Lee, J.-H., Moon, C.-K., Brütting, W., and Kim, J.-J. (2013). Organic light-emitting diodes with 30% external quantum efficiency based on a horizontally oriented emitter. *Adv. Funct. Mater.* 23, 3896–3900.
84. Chen, C.-Y., Lee, W.-K., Chen, Y.-J., Lu, C.-Y., Lin, H.Y., and Wu, C.-C. (2015). Enhancing optical out-coupling of organic light-emitting devices with nanostructured composite electrodes consisting of indium tin oxide nanomesh and conducting polymer. *Adv. Mater.* 27, 4883–4888.
85. Tong, B., Mei, Q., Chen, D., and Lu, M. (2012). Synthesis and electroluminescent properties of red emissive iridium(III) complexes with ester-substituted phenylquinoline ligands. *Synth. Met.* 162, 1701–1706.